

Changes in hydrogen bonding in protein plasticized with triethylene glycol

Talia Maree Hicks,¹ Casparus Johannes Reinhard Verbeek,¹ Mark Christopher Lay,¹ Merilyn Manley-Harris²

¹School of Engineering, Faculty of Science and Engineering, University of Waikato, Hamilton 3240, New Zealand

²School of Science, Faculty of Science and Engineering, University of Waikato, Hamilton 3240, New Zealand

Correspondence to: T. M. Hicks (E-mail: tmh20@students.waikato.ac.nz)

ABSTRACT: Bloodmeal decolored with 4 wt % peracetic acid can be extruded into a semi-transparent bio-plastic through the addition of sodium dodecyl sulfate (SDS), water, and triethylene glycol (TEG). TEG is often used to plasticize protein thermoplastic materials because of its ability to form both hydrophobic and hydrogen bonds. Synchrotron-based FT-IR was used to monitor changes in the types of hydrogen bonding occurring in TEG plasticized protein during heating. Heating was found to overcome a portion of the weaker hydrogen bonds found within and between proteins, observed as a blue-shift in the N-H and O-H stretching vibrations occurring at $\sim 3280\text{ cm}^{-1}$. TEG was shown to be involved in a larger array of hydrogen bonding environments after heating, evidenced by the broadening of the C-OH stretch around 1076 cm^{-1} , suggesting improved plasticizer-protein interactions. Additionally, these bonds were found to be as strong as the original interactions, observed as a shift in the C-OH peak back to its original wavenumber ($\sim 1076\text{ cm}^{-1}$) during cooling. Initially, TEG was spatially distributed into distinct plasticizer-rich and plasticizer-poor domains, giving rise to two glass transitions. Heating allowed the migration and uniform dispersion of TEG throughout the material, and merged the two glass transitions into one broader glass transition region. Heating during DSC removed the peak around 60°C corresponding to the enthalpy of relaxation, which is associated with physical aging of amorphous and semi-crystalline polymers. While physical aging occurred during the storage of DBM, in the presence of TEG it occurred to a lesser extent. © 2015 Wiley Periodicals, Inc. *J. Appl. Polym. Sci.* 2015, 132, 42166.

KEYWORDS: biopolymers & renewable polymers; properties and characterization; proteins; spectroscopy

Received 24 December 2014; accepted 26 February 2015

DOI: 10.1002/app.42166

INTRODUCTION

Bloodmeal, a by-product of the meat industry, can be decolored using 4 wt % peracetic acid. The resulting pale-yellow material can be extruded into a semi-transparent bio-plastic by adding sodium dodecyl sulfate (SDS), water, and triethylene glycol (TEG).¹

Proteins tend to have a high glass transition and melting temperature, typically higher than the temperature at which degradation occurs. To avoid thermal degradation plasticizers are used to lower the glass transition temperature (T_g).²

Oxidative decoloring with peracetic acid breaks disulfide bonds present in bloodmeal and reduces the number of other stabilizing interactions³ resulting in a more soluble material with a lower T_g .⁴ Despite this, the addition of SDS and TEG are also required to impart sufficient mobility of the proteins during extrusion.⁵

In addition to SDS and TEG, the pre-extruded mixture also contains water, which is often used to plasticize protein-based thermoplastics. However, during heating and storage significant evaporation can occur, resulting in embrittlement of the material. To prevent this, less volatile plasticizers are often used alongside or instead of water. Tri-ethylene glycol (TEG) has been shown to be an effective plasticizer in bloodmeal-based thermoplastics⁶ and in decolored bloodmeal (DBM).^{1,5,7}

During extrusion, creating a homogeneous blend of components in the melt is of paramount importance to obtaining a consolidated product. Adequate dispersion of plasticizer is required, and involves wetting and adsorption followed by solvation and/or penetration into the protein. Adsorption and diffusion of the plasticizer may not necessarily result in even distribution and is dependent on both the type of plasticizer used and the amino acids in the protein.^{8,9}

In protein-based thermoplastics, polyol plasticizers have been found to be most effective because they contain both polar and nonpolar groups which are able to hydrogen bond and interact hydrophobically with protein chains,⁹ which may lead to lower rates of leaching compared to polar plasticizers urea and water.

Plasticizer distribution in the feedstock and melt has implications during processing and on the resulting material properties. For instance, if the plasticizer concentration is too high in the feedstock, it can exceed the compatibility limit and lead to phase separation.¹⁰ Phase separation into regions of high and low plasticizer concentration has been implicated in the presence of two glass transitions in soy protein-based plastics¹¹ and in bloodmeal protein-based thermoplastic.¹²

The purpose of this article was to investigate how heating disrupted stabilizing hydrogen bonding interactions within and between proteins and facilitated the migration and dispersion of TEG. This would give a greater understanding of how temperature affects hydrogen bonding dynamics which can be used to further optimize processing conditions for extrusion and injection moulding. Synchrotron-based FT-IR was used to monitor changes in hydrogen bonding interactions between proteins and plasticizer during heating. The distribution of TEG throughout the DBM particles before, during and after heating was monitored via peaks corresponding with the alcohol and ether groups in the TEG molecule.

METHODOLOGY

Reagents

Bovine bloodmeal was obtained from Wallace Corporation, New Zealand, and sieved to utilize particles under 710 μm . Peracetic acid (Proxitane Sanitizer 5%) was purchased from Solvay Interlox Pty, Auckland, New Zealand. Sodium dodecyl sulfate (Thermo Fisher Scientific, Loughborough, UK) and triethylene glycol (Merck Millipore, Auckland, New Zealand) were dissolved in distilled water for addition to decolored bloodmeal.

Sample Preparation

Bloodmeal was decolored by adding 4 wt % peracetic acid solution (300 g) to bloodmeal (100 g) and reacted during high speed mixing (10 min) in a Kenwood Cooking Chef KM080 mixer with the creaming beater attachment to ensure homogeneous decoloring.³ This mixture was diluted with distilled water (300 g) and immediately neutralized with $\sim 1 \text{ mol L}^{-1}$ sodium hydroxide and filtered. The decolored bloodmeal was oven dried overnight (75°C) to approximately 2–4 wt % moisture and milled to $< 1 \text{ mm}$.

Samples were prepared by dissolving SDS (0.6 g) in 10 g distilled water (50°C), and mixing with decolored bloodmeal (20 g) for 10 minutes using a hand-held Omni International Tissue Homogenizer set with a hard-tissue plastic generator probe. For samples containing plasticizer, 4 g of triethylene glycol was added to the SDS DBM blend, followed by an additional 10 minutes mixing. The resultant mixtures were stored overnight in sealed plastic containers below 4°C, followed by freeze-drying (48 h) in a Labconco FreeZone 2.5 L Benchtop Freeze Dry System. Final moisture content was determined using thermogravimetric analysis. Samples used for synchrotron

FT-IR analysis contained $\sim 2\text{--}4 \text{ wt } \%$ moisture. Moisture content was found to have increased to 8 wt % during storage prior to DMA and DSC analysis.

Synchrotron FT-IR Microscopy

Spatially and thermally resolved FT-IR experiments were undertaken on the infrared microspectroscopy beamline at the Australian Synchrotron, Victoria, Australia. Individual particles of decolored bloodmeal (DBM) and DBM with additives were compressed in a diamond cell and then transferred to a barium fluoride slide. This was placed in a Linkam temperature controlled stage connected to a Bruker Hyperion 3000 with an MCT collector and XY stage. The stage was set to 24°C and purged with nitrogen gas. Thirty-two spectra were collected in transmission mode with a resolution of 4 cm^{-1} between 3900 and 700 cm^{-1} and averaged using Opus 7.2 software (Bruker Optik GmbH 2013).

Three types of experiments were performed to determine the effect of thermal treatment on the pre-extruded material: (1) thermally resolved, (2) spatial mapping before and after thermal treatment, and (3) spatial mapping throughout thermal treatment using isothermal holds.

Thermally Resolved FT-IR. A $10 \times 10 \mu\text{m}$ spot within the center of each compressed particle was chosen and spectra collected at 30-s intervals during a constant heating ramp from -60°C to 120°C at 2°C min^{-1} .

Spatial Mapping Before and After Thermal Treatment. Each compressed particle was mapped using a $10 \times 10 \mu\text{m}$ spot size chosen on video images at 24°C and a map containing ~ 100 points was obtained. After mapping, the mounted sample was heated at $50^\circ\text{C min}^{-1}$ in the Linkam stage to 120°C , held isothermally for 2 min then cooled back to room temperature at $50^\circ\text{C min}^{-1}$. A grid with the same *xy* co-ordinates as the original scan was then mapped for a second time. For each sample type, three separate particles were mapped and scanned.

Spatial Mapping During Thermal Treatment Using Isothermal Holds. A compressed particle of DBM with processing aids was mounted and a $\sim 60 \times 60 \mu\text{m}$ grid was chosen using a $10 \times 10 \mu\text{m}$ spot size. Grids with the same *xy* co-ordinates were scanned at the following temperatures; $\sim 24^\circ\text{C}$, 45°C , 55°C , 75°C , 100°C , and 120°C . Heating was carried out at $50^\circ\text{C min}^{-1}$ to each successive temperature, and the sample allowed to equilibrate for 10 minutes before mapping. For each sample type, three separate particles were scanned.

Data and Statistical Analysis

FT-IR spectra for each point were integrated for obtaining the thermally resolved and spatial maps of triethylene glycol to amide III peak area ratios using OPUS 7.2. Opus type B integrals were calculated from 1150 to 1045 cm^{-1} (C-O-C and C-OH functional groups in TEG) and from 1330 to 1180 cm^{-1} (amide III region of proteins), along with the ratio of the first peak over the second,¹² to eliminate the effects of variation in thickness across the sample. These ratios were used to compare TEG distribution relative to protein in spatial maps. A comparison of the C-O-C and C-OH peak areas to each other was determined to discern changes in hydrogen bonding

environment, this was achieved by integrating using an Opus type B integral from 1150 to 1090 cm^{-1} (C-O-C) and from 1090 to 1045 cm^{-1} (C-OH) to obtain the ratio of the second peak over the first. Mean, standard deviation, and corresponding histograms were calculated for the mapped ratios. Two additional peaks unique to triethylene glycol (960–905 and 905–860 cm^{-1}) were also compared to the peak area of the amide III region to determine the accuracy of using the C-O stretches of TEG to determine relative changes in TEG content. Data were filtered for a minimum area under the amide III region to exclude points mapped outside particles from statistical analysis.

Thermogravimetric Analysis

Mass loss of DBM samples (~ 10 mg) in a 0.9 g ceramic crucible were recorded during heating in dry air at $10^\circ\text{C min}^{-1}$ to 800°C in a Texas Instruments SDT 2960 analyzer. Moisture content was determined from the cumulative mass loss up to 120°C .

Dynamic Mechanical Analysis

DMA was performed using a Perkin Elmer DMA 8000 fitted with a high-temperature furnace and cooled with liquid nitrogen. DBM samples were examined by mounting ~ 50 mg of powder in $1.0 \times 7.4 \times 28$ mm (folded dimensions) material pockets (Perkin Elmer) and tested at 0.1, 0.3, 1, 3, 10, and 30 Hz with a dynamic displacement of 0.05 mm and free length of 12.5 mm. Decolored bloodmeal samples containing TEG were analysed in two ways: (1) heating from -60°C to 250°C and (2) heating from -60°C to 120°C to remove thermal history before heating from -60°C to 250°C .

Differential Scanning Calorimetry

DSC was conducted in a Perkin Elmer DSC 8500 hyper DSC fitted with an autosampler accessory and cooled with liquid nitrogen. Approximately 5–10 mg of sample was weighed into 30 μL aluminium autosampler pans (Perkin Elmer) which were then crimped to provide a seal and placed into the auto sampler. All samples were scanned between 0°C and 120°C at $10^\circ\text{C min}^{-1}$ and cooled to 0°C at the same rate before performing a second scan under the same conditions. Glass transition temperature (half C_p extrapolated) was determined from the second scan using Pyris 7 software (Perkin Elmer).

RESULTS AND DISCUSSION

Triethylene glycol is an aliphatic dihydroxy alcohol containing two ether linkages (Figure 1 insert), which strongly absorbs infrared between 1150–1090 cm^{-1} and 1090–1045 cm^{-1} giving rise to two similar sized peaks (Figure 1). The first peak is assigned to the asymmetric stretching vibration of the aliphatic ether groups, ($\nu_{as}\text{C-O-C}$) and the second peak is attributed to the stretch of the primary alcohol groups ($\nu\text{C-OH}$). Two smaller peaks unique to TEG are also observed, occurring at 960–905 and 905–860 cm^{-1} . Assignment of these peaks is difficult as they are caused by coupling of several vibrational modes such as the ether symmetric stretch ($\nu_s\text{C-O-C}$), out of plane C-OH bends, C-C stretches, and C-H out of plane bending within the rest of the molecule. These characteristic peaks were only observed in DBM samples containing TEG and were used to

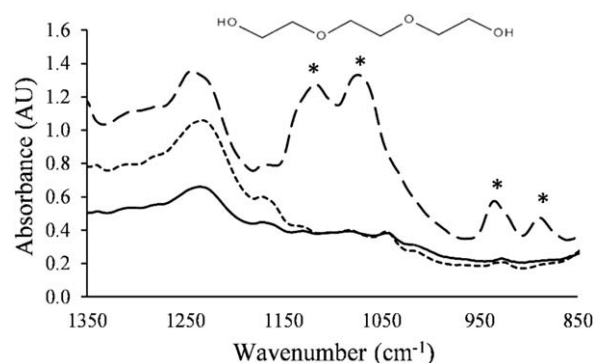


Figure 1. FT-IR absorbance spectrum of decolored bloodmeal (DBM) (—), DBM containing sodium dodecyl sulfate (DBM SDS) (---), and DBM containing SDS and triethylene glycol (DBM TEG) (- -) indicating the absorbance of TEG peaks (*) and the amide III region (1180–1330 cm^{-1}). Insert: structure of triethylene glycol.

monitor changes in TEG content relative to the amide III region (Figure 1).

The main hydrogen bonding interactions taking place within DBM containing TEG include those formed through intra- and intermolecular protein interactions, TEG–protein interactions and intra- and intermolecular TEG–TEG interactions. A recent frontier orbital study has indicated that the alcohol groups of triethylene glycol are most energetically stable when accepting hydrogen bonds from other molecules such as water, resulting in shorter O...H bond distance, greater interaction energy, and a higher degree of charge transfer compared to when it acted as a hydrogen bond donor.¹³ Accordingly, it is most likely that TEG will preferentially act as a hydrogen bond acceptor in the presence of other hydrogen bond donors such as water and protein. Typically, hydrogen bonding is diminished with increasing temperature, but it is possible only some of the weaker bonds are overcome leaving the stronger bonds intact.

Thermally Resolved FT-IR

A single location on a DBM particle was scanned every 30 s using a $10 \times 10 \mu\text{m}$ aperture during a heating cycle (-60°C to 120°C at 2°C min^{-1}). Heating was found to increase the absolute absorbance within each spectra (Figure 2), and were normalized at 2874 cm^{-1} (asymmetric stretching of CH_3) prior to comparison. Heating from room temperature to 120°C led to an increase in intensity in both the amide III region and each of the TEG peaks (Figure 2). In addition to increased absorption, the amide III region changed shape dramatically, gaining intensity around 1306 and 1228 cm^{-1} , and has been attributed to the formation of α -helices and β -sheets during heating.⁵

The peak around 1074.2 cm^{-1} associated with the carbon–oxygen stretch of the TEG primary alcohol groups ($\nu\text{C-OH}$) red-shifted and broadened with increasing temperature, and by 120°C had shifted to 1070.4 cm^{-1} . As a general rule, hydrogen bonding lowers the frequency of stretching vibrations for the functional group involved because of a reduction in the force constant associated with the X-H covalent bond.¹⁴ However, literature investigating the effects of hydrogen bonding (via solvation and temperature) on the position of the C-O band for

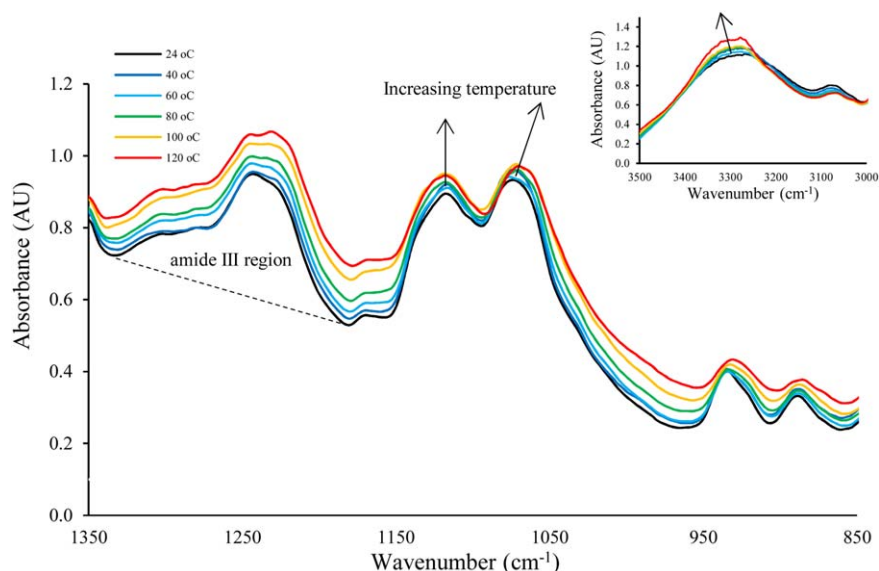


Figure 2. Normalized FT-IR absorbance spectrum of decolorized bloodmeal with sodium dodecyl sulfate and triethylene glycol (DBM TEG) with increasing temperature. Insert: Absorbance from 3500 to 3000 cm^{-1} showing the νOH peak with increasing temperature. FT-IR Normalized to 1 AU at 2874 cm^{-1} . [Color figure can be viewed in the online issue, which is available at wileyonlinelibrary.com.]

aliphatic alcohols is sparse.¹⁵ The shift in this peak to lower wavenumber with increasing temperature is caused by a reduction in the C-O force constant (increased C-O bond length). The increase in the C-O bond length results from a lower degree of shared electron density between the alcohol oxygen and the hydrogen donor. The broadening of this peak, however, indicates a greater variety of hydrogen bonding interactions are taking place between TEG and other species, perhaps an indication of improved interaction with the protein.

Another indicator of the changing dynamics during heating is the indistinguishable $\nu\text{O-H}$ and $\nu\text{N-H}$ bands that are also sensitive to their chemical environment. Like N-H, the stretching vibration for O-H generally appears at $\sim 3200 \text{ cm}^{-1}$ in a concentrated solution or solid sample (appearing near $\sim 3600 \text{ cm}^{-1}$ in dilute or weakly hydrogen bonded samples). Hydrogen bonding (X---O-H) increases the length of the covalent O-H-bond (reducing the force constant and the frequency of IR absorption). In addition, H-bonded hydroxyl groups tend to show reduced absorbance intensity and broadened stretching frequency.

For DBM containing TEG, the νOH (and νNH) band is situated around 3280 cm^{-1} and was found to become sharper with increasing temperature (Figure 2). The sharpening of this peak reflects a reduction in the overall variety of hydrogen bonds taking place as the temperature increased, a result of thermal energy overcoming weak H-bonds.

Hydrogen bond energies range from 1 to 4 kcal mol^{-1} for weak bonds through to $\sim 15\text{--}40 \text{ kcal mol}^{-1}$ for strong bonds.¹⁶ Intramolecular H-bonds in ethylene glycol derivatives are comparatively larger ($\sim 13.7\text{--}15.9 \text{ kcal mol}^{-1}$)¹⁷ than intramolecular H-bonding in proteins ($\sim 6\text{--}8 \text{ kcal mol}^{-1}$ for N-H---O=C and $\sim 1.5\text{--}1.8 \text{ kcal mol}^{-1}$ for $\text{C}_\alpha\text{-H---O=C}$ interactions¹⁸). The observed blue-shift from ~ 3280 to 3290 cm^{-1} upon heating

suggests that the N-H and O-H groups in the sample are located within weaker or non H-bonded environments.¹⁹

Considering both the observed shifts ($\nu\text{N-H}$ and $\nu\text{O-H}$ and that of $\nu\text{C-OH}$) the overall number of hydrogen bonds within the sample was reduced during heating, observed as the narrowing of the $\nu\text{N-H}$ and $\nu\text{O-H}$ band which also shifted to higher frequency. Estimated values of the hydrogen bonding energies for proteins and ethylene glycol derivatives suggest this change predominantly involves bonding within and between the proteins. Although TEG hydrogen bonding interactions were also weakened overall, TEG was found to take part in a larger variety of interactions during heating, observed as broadening of the $\nu\text{C-OH}$ peak.

The hydrogen bonding environment in a material is strongly affected by temperature and concentration of molecules capable of forming hydrogen bonding interactions. FT-IR has revealed the hydrogen bonding environment of TEG changes during heating, which may be in part because of the evaporation of TEG. The area associated with TEG specific peaks relative to the area of the amide III region was monitored throughout heating, and decreased, despite the increase in overall intensity of the full spectra during heating (Figure 2). The area of the amide III region remained reasonably constant throughout heating, whereas a reduction in the area of all TEG-related peaks was observed (Figure 3).

Triethylene glycol has a high boiling point (288°C) and a low vapor pressure, ideal for use as a plasticizer in thermoplastics as it is less likely to evaporate under standard temperatures used for thermoplastic processing of proteins. Thermogravimetric analysis of DBM and DBM containing TEG showed similar mass loss profiles between 25°C and 120°C , appearing to lose $\sim 1.5\text{--}2.5 \text{ wt } \%$ between 80°C and 120°C , this is most likely in the form of water but may also contain TEG (Figure 4).

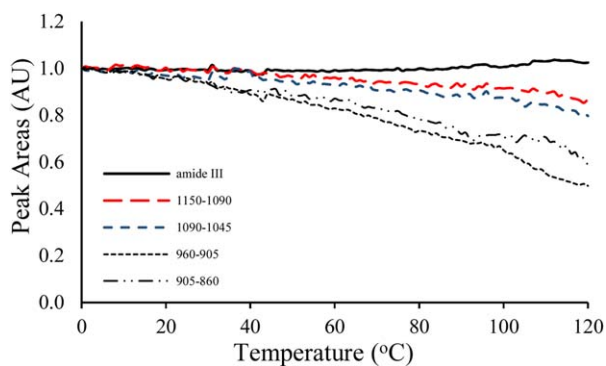


Figure 3. Normalized peak area of the amide III region and each of the TEG peaks with increasing temperature. [Color figure can be viewed in the online issue, which is available at wileyonlinelibrary.com.]

The larger mass loss event occurred from $\sim 150^{\circ}\text{C}$ to 250°C could correspond with the evaporation of TEG, as it is not observed in its absence. While minor quantities of TEG may evaporate during heating, it is possible the change observed in Figure 3 is a result of the TEG migrating out of the $10 \times 10 \mu\text{m}$ spot being scanned, and was further investigated by determining the spatial distribution of TEG prior to and after rapid heating.

Spatial Distribution of TEG

The relative TEG content was measured as a ratio of the area between 1150 and 1045 cm^{-1} to the amide III area between 1330 and 1180 cm^{-1} (TEG : amide III ratio). Prior to heating, TEG content across the particles appeared to be normally distributed (Figure 5), with no statistical difference in TEG content between the perimeter and the core of the particle. After heating, the TEG content is significantly reduced ($P < 0.01$)

Despite an apparent normal distribution of TEG throughout the DBM, the spatial distribution indicated the formation of plasticizer-rich (high ratio) and plasticizer-poor (low ratio) domains uniformly scattered throughout an otherwise homogeneous matrix [Figure 6(A)]. Both the TEG-rich and TEG-poor domains were found to be statistically different to the average composition of the sample ($P < 0.01$).

The distribution of TEG-rich and TEG-poor domains may be a result of porosity in the DBM feedstock leading to adsorption of TEG in layers within the cavities and diffuses only partially into the protein. However, it is much more likely that the concentration of TEG in DBM exceeded the compatibility limit of the protein resulting in phase separation, often observed as plasticizer exclusion in biopolymer materials.¹⁰

TEG distribution was found not to correlate with secondary structure distribution,⁵ indicating that TEG interacts with protein structures at a primary structure level indiscriminately. Therefore, the observed distribution of TEG is not caused by preferential localization in hydrophilic or hydrophobic areas of the protein.

After the application of the heat-cool cycle (simulating the residence time of an extruder), spatial maps indicated an approximate 14% loss in TEG, equivalent to 2.3 wt % total mass loss,

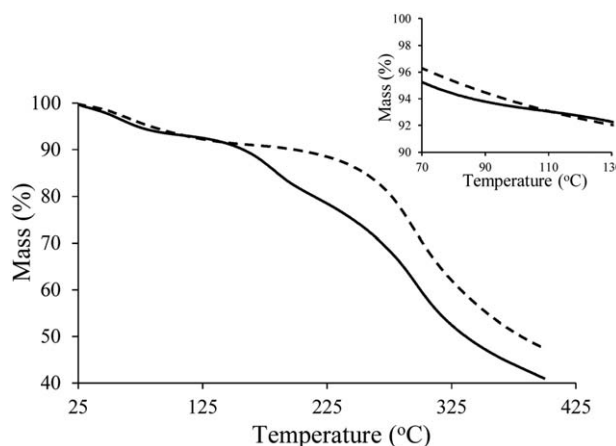


Figure 4. Thermogravimetric analysis of decolorized bloodmeal (DBM) (---) and decolorized bloodmeal containing sodium dodecyl sulfate and triethylene glycol (DBM TEG) (—) carried out at $10^{\circ}\text{C min}^{-1}$. Insert: Mass loss occurring between 70°C and 130°C .

along with a reduction in the variation of TEG content throughout the particle. The distribution of TEG was found to be more homogenous, evidenced by a reduction in standard deviation and range of the TEG : amide III peak area ratio [Figure 6(B)]. Improved homogeneity could be caused by both the evaporation of phase-separated TEG (from areas initially rich in TEG) as well as by the migration of TEG throughout the particles because of thermally induced diffusion.

An interesting observation is the small but statistically significant increase in the $\nu\text{C-OH}$ to $\nu\text{C-O-C}$ ratio upon heating and cooling ($P < 0.01$) (Figure 7). Their peak shape and their position are thought to be related to their hydrogen bonding environment, as discussed earlier. This was explored further using spatial mapping after isothermal holds at different temperatures to allow thermal equilibration.

The increase in the ratio of $\nu\text{C-OH}$ to $\nu\text{C-O-C}$ is caused by the increase in the area of the alcohol C-O stretch in TEG. After heating, the spatial variation is still heterogeneous, with approximately the same standard deviation and range. Despite this, the increase in the mean ratio (because of increase in $\nu\text{C-OH}$ area) reflects the increased variety of hydrogen bonding interactions TEG is involved with after heating, which is a good indicator

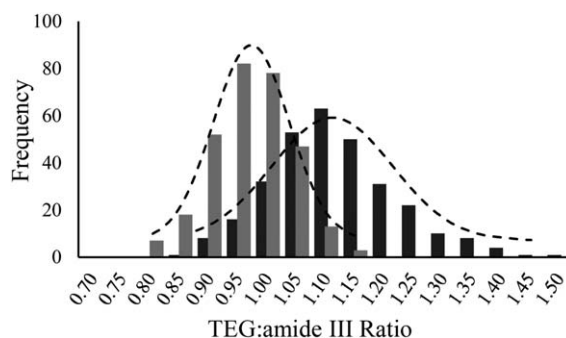


Figure 5. Histogram for distribution of TEG through decolorized bloodmeal prior to heating (■) and after heat-cool cycle (■).

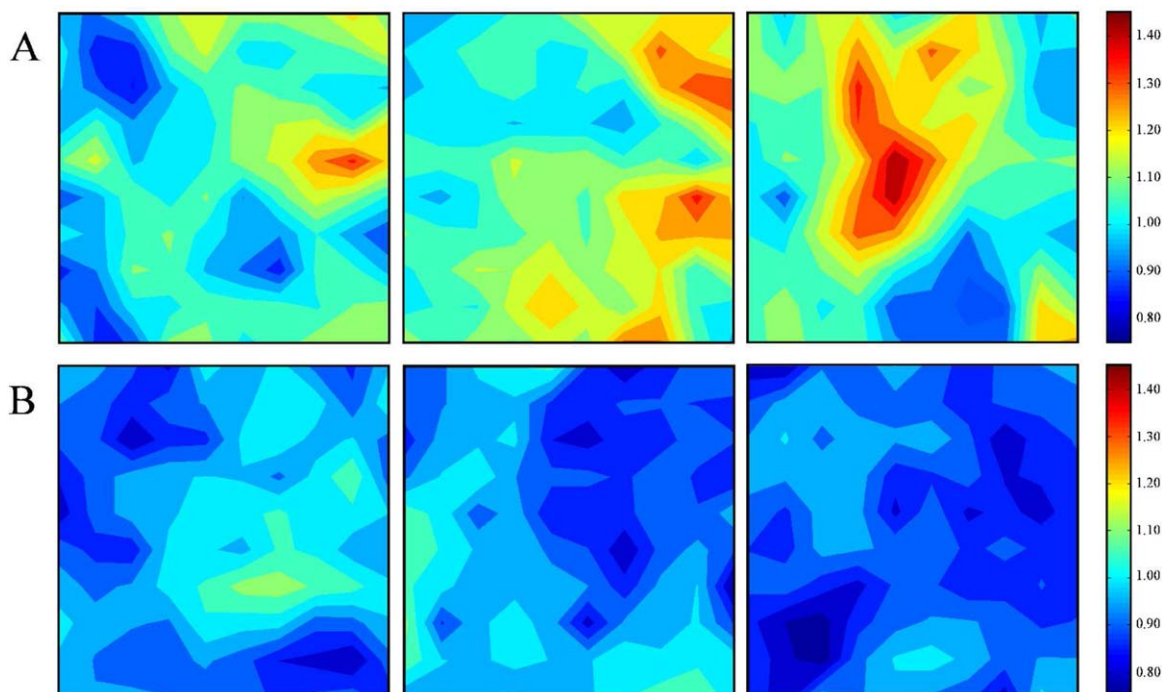


Figure 6. Spatial map of the ratio of triethylene glycol (TEG) to amide III region, showing the distribution of plasticizer throughout the decolored bloodmeal particle as three $10 \times 10 \mu\text{m}$ grids, i.e. $N = 300$. (A) Distribution of TEG prior to heat cycle, (B) distribution of TEG after heat cycle and cooling to room temperature. [Color figure can be viewed in the online issue, which is available at wileyonlinelibrary.com.]

that TEG is interacting with more protein groups after heating. Furthermore, the $\nu\text{C-OH}$ peak position that was shown to decrease during heating (Figure 2), reverts back to its original wavenumber (1076.2 cm^{-1}) upon cooling.

Spatial Mapping During Thermal Treatment Using Isothermal Holds

During preparation of the thermoplastic feedstock, TEG diffuses through the protein, forming heterogeneous regions of high and

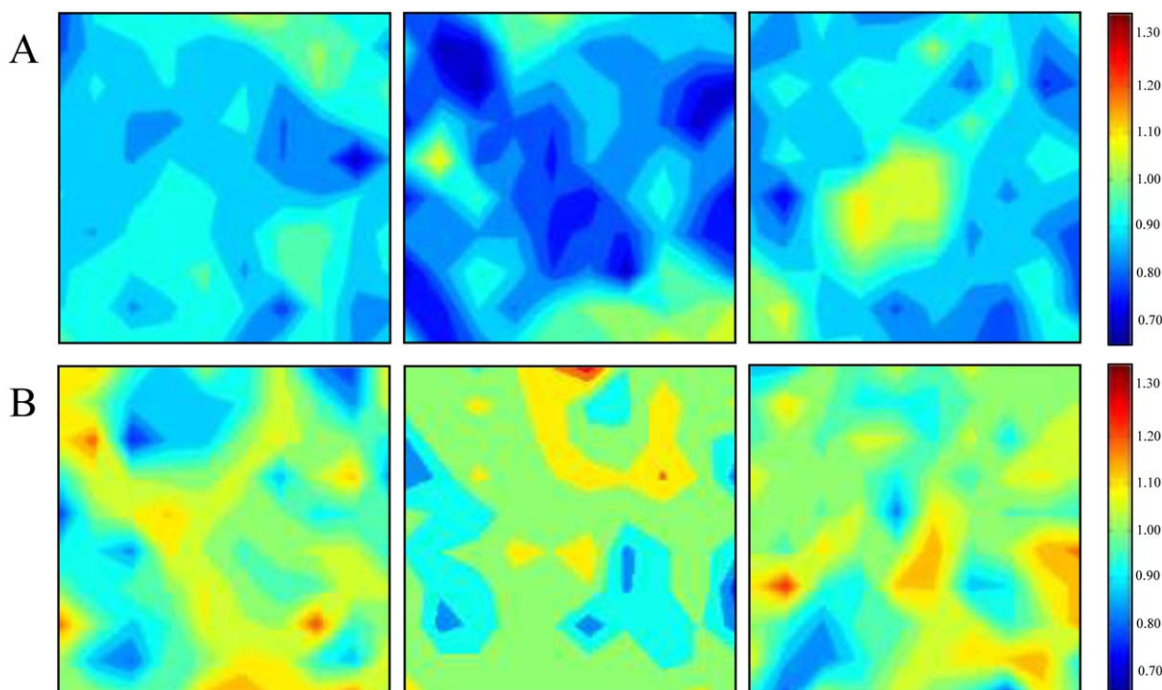


Figure 7. Spatial distribution of the $\nu\text{C-OH}$ to $\nu\text{C-O-C}$ peak area ratio for DBM containing sodium dodecyl sulfate and triethylene glycol (DBM TEG) at room temperature (A) before heating (mean = 0.88, $\sigma = 0.09$) and (B) after heat cycle and cooling to room temperature (mean = 1.02, $\sigma = 0.10$). [Color figure can be viewed in the online issue, which is available at wileyonlinelibrary.com.]

Table I. Summary of Statistics for the Peak Area Ratio of ν C-OH to ν C-O-C for Spatial Maps of DBM Containing SDS and TEG During Heating

| | ν C-OH: ν C-O-C ratio | | |
|-----------------------|-------------------------------|-----------|-------|
| | Total | Perimeter | Core |
| 24°C | | | |
| Mean | 0.99 | 0.95 | 1.01 |
| Std. deviation | 0.15 | 0.20 | 0.10 |
| T-test P vs C | | 0.10 | |
| 45°C | | | |
| Mean | 0.99 | 0.93 | 1.03 |
| Std. deviation | 0.16 | 0.21 | 0.14 |
| T-test 24°C vs 45°C | 0.92 | 0.60 | 0.50 |
| T-test P vs C | | 0.00* | |
| 55°C | | | |
| Mean | 1.00 | 0.96 | 1.04 |
| Std. deviation | 0.13 | 0.17 | 0.08 |
| T-test 45°C vs 55°C | 0.59 | 0.45 | 0.60 |
| T-test P vs C | | 0.00* | |
| 75°C | | | |
| Mean | 1.01 | 0.98 | 1.04 |
| Std. deviation | 0.13 | 0.16 | 0.09 |
| T-test 55°C vs 75°C | 0.49 | 0.49 | 0.76 |
| T-test P vs C | | 0.00* | |
| 100°C | | | |
| Mean | 1.03 | 0.96 | 1.09 |
| Std. deviation | 0.20 | 0.24 | 0.14 |
| T-test 75°C vs 100°C | 0.49 | 0.70 | 0.05 |
| T-test P vs C | | 0.00* | |
| 120°C | | | |
| Mean | 1.12 | 1.08 | 1.16 |
| Std. deviation | 0.22 | 0.24 | 0.21 |
| T-test 100°C vs 120°C | 0.00* | 0.02* | 0.06 |
| T-test 24°C vs 120°C | 0.00* | 0.00* | 0.02* |
| T-test P vs C | | 0.10 | |

Statistically significant results are marked * ($P < 0.05$)

low plasticizer content. A well-consolidated material requires uniform distribution of plasticizer, and relies on having overcome any immediate interactions to provide mobility allowing migration to new areas where new stabilizing interactions can form. The on-set of this phenomenon was determined during incremental increases in temperature, allowing enough time for thermal equilibration.

Below 100°C, the average relative peak area of ν C-OH to ν C-O-C showed no statistical difference before and after thermal treatment. No difference between maps obtained at 120°C, and those obtained upon cooling from 120°C was observed, indicating the change to ν C-OH area was permanent. This suggests that the sample must surpass 100°C in order for the TEG to create new hydrogen bonding interactions in any significant amount (Table I), and that they remain upon cooling.

Prolonged heating at elevated temperature caused a small loss in TEG and an irreversible change in the types of intermolecular hydrogen bonding with which TEG is involved. However, there was no correlation between TEG content with secondary structure distribution.

FT-IR analysis indicated the occurrence of several important structural changes that take place during heating. Heating resulted in reduced stabilizing hydrogen bonding interactions within the protein, evidenced by the narrowing of the peak around 3290 cm^{-1} . The results from Figures 3 and 4 suggest evaporation accounts for ~14% of TEG, a total mass loss of 2.3 wt %. Finally, the TEG was shown to migrate, and partake in a larger variety of hydrogen bonding interactions, evidenced through improved distribution after heating, a larger ν C-OH peak area which shifts back to its original wavenumber (1076.2 cm^{-1}) upon cooling.

Dynamical Mechanical Analysis

Upon cooling, FTIR showed a reduction in the variation of TEG content across the samples, with less extreme localized domains. Initially, these two domains were sufficiently different in material properties to give rise to what appeared to be two distinct glass transitions in DMA, which after heating were found to merge, reflecting improved homogeneity.

DBM and DBM with TEG containing ~8 wt % moisture were scanned from -60°C to 250°C before and after removing thermal history to investigate the effect of SDS and TEG and thermal treatment on material behavior. DBM showed two peaks in $\text{Tan } \delta$, allocated to a T_g (75°C), and a transition owing to a T_g of dehydrated protein coupled with the onset of protein degradation (220°C) which is observed at the same temperature in both scans (Figure 8).

Preheating DBM to 120°C largely removed the peak around 75°C (smoothing it out), and may be attributed to the relaxation associated with aging of amorphous polymers, as a similar effect is observed during DSC.

The shift of glass transition temperature with frequency follows an Arrhenius relationship ($\log_{10} K \propto 1/T$) and is generally used to estimate the activation energy of the transition by plotting the log of the DMA frequency employed against the inverse of the absolute temperature at which the loss modulus peak occurs. The Arrhenius plot for DBM confirmed that the first transition around 75°C is a result of two overlapping events, as in the first scan it is not linearly proportional to the frequency applied, but becomes so if the thermal history is first removed by preheating to 120°C (Figure 9).

Upon addition of TEG, DMA showed three relaxation events, the first occurring below 0°C which may be because of frozen water melting as the sample was heated. The second and third peaks may both be glass transitions, caused by the TEG-rich and TEG-poor domains found in DBM with TEG. Thermal pre-treatment merges these peaks into one broader peak with the removal of the sub-zero transition. The Arrhenius plot confirmed this, indicating that both peaks occurring around 50°C and 115°C in the first scan are linear with respect to log frequency, strongly suggesting they are both the result of a glass

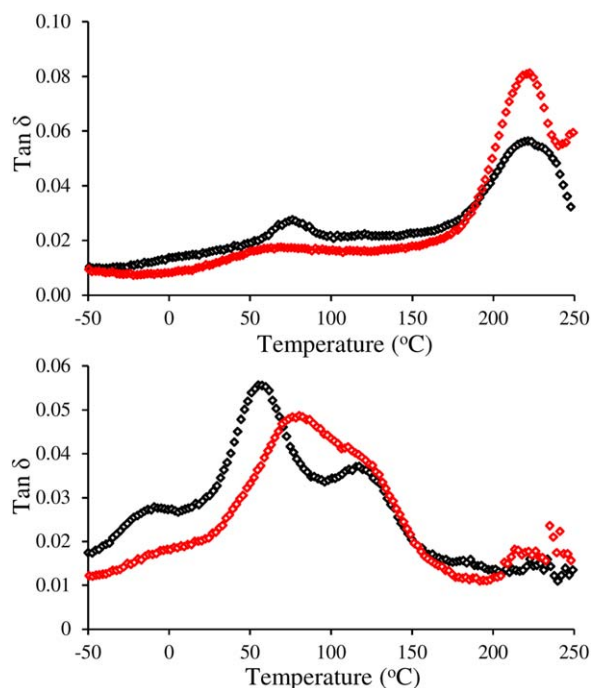


Figure 8. DMA of decolorized bloodmeal: (A) DBM, (B) DBM with sodium dodecyl sulfate and triethylene glycol (DBM TEG). Without removing thermal history (\blacklozenge) and after removing thermal history (\diamond) by preheating to 120°C. [Color figure can be viewed in the online issue, which is available at wileyonlinelibrary.com.]

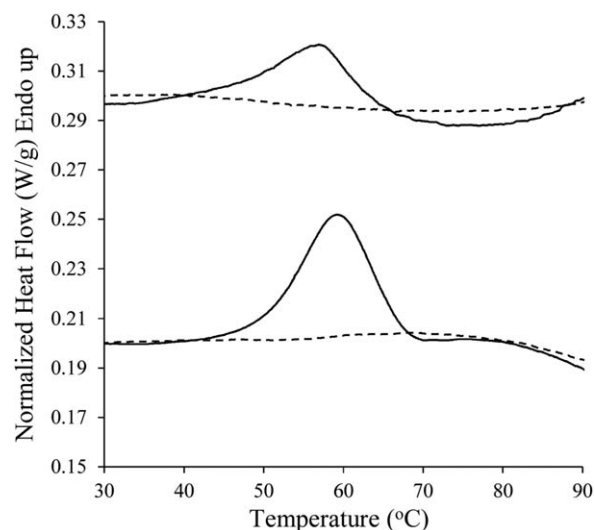


Figure 10. DSC thermograms of decolorized bloodmeal (DBM) and DBM with sodium dodecyl sulfate and triethylene glycol (DBM TEG). Scans were carried out using a heating rate of 10°C min⁻¹. First scan solid line (—) and second scan dashed line (- -). Images have been stacked for clarity.

transition. Removing the thermal history (pre-heating to 120°C) also led to a linear response in the peak around 60°C and the position of the shoulder at around 115°C, indicating the lower temperature transition has increased in temperature as TEG has migrated slightly to become more homogeneously distributed after heating.

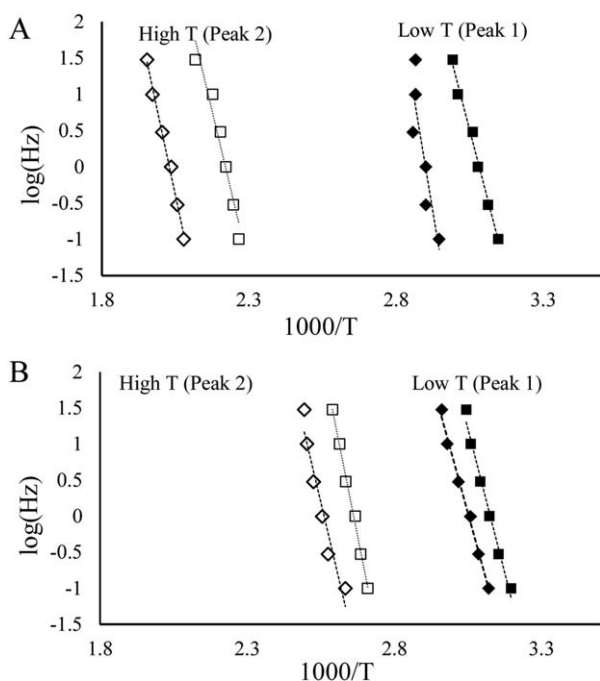


Figure 9. Arrhenius plot for A: DBM and B: DBM with SDS and TEG. Low temperature transition scan 1 (\blacklozenge) (R^2 values A = 0.7601, B = 0.9932) and Scan 2 (\blacksquare) (R^2 values A = 0.9888, B = 0.9837) and high temperature transition scan 1 (\diamond) (R^2 values A = 0.9931, B = 0.9368) and scan 2 (\square) (R^2 values A = 0.9467, B = 0.9956). Plots are stacked for clarity.

Physical Aging

DSC showed the presence of two overlapping thermal events occurring at 75°C. During heating to 120°C (to remove thermal history), the close packing that occurred during aging was lost. Physical aging is a phenomenon observed when an amorphous polymer is stored below its glass transition temperature,²⁰ under which material will have a free volume, enthalpy and entropy larger than it would have under equilibrium.²¹ As a result, the nonequilibrium material undergoes slow chain rearrangement (through short-range, rotational reorientations) toward an equilibrium conformation, a process known as physical aging.²²

When an aged polymer is heated above its T_g , it absorbs the heat lost during aging and recovers its lost free volume and this is accompanied by the development of an endothermic peak at its glass transition, observed during DSC.²⁰ This phenomenon has also been reported for numerous polymers and proteins.^{20,23,24} The presence of this sub- T_g endothermic event was observed during DSC of DBM with and without TEG, Figure 10.

Initially the specific enthalpy for DBM was 2.8 J g⁻¹ and decreased to 1.5 J g⁻¹ after the addition of TEG. The addition of TEG reduced the degree to which aging can occur as observed as a reduction in the enthalpy of relaxation, also reducing the temperature at which it occurred. This may be because of TEG forming competing interactions with protein that reduce the ability of protein chains to form hydrogen bonds and other intermolecular interactions which facilitate close packing, increasing free volume. These endothermic peaks are no longer

observed upon reheating the material, suggesting that the event occurring during DSC is the same as the one which had occurred during DMA, where TEG is unable to evaporate.

CONCLUSION

Sorption of TEG into DBM protein led to two distinct domains: one plasticizer-rich and the other plasticizer-poor, distributed throughout an otherwise homogeneous blend. The two regions were found to be distinctly different in TEG concentration and also in their thermal behavior, resulting in two glass transitions.

Several important structural changes were found to take place during heating. First, heating resulted in reduced stabilizing hydrogen bonding interactions within the protein. Although a minor amount of evaporation occurred during FT-IR, the TEG was shown to migrate throughout the sample, and more importantly was shown to partake in a greater variety of hydrogen bonding interactions, evidenced by the permanent increase in the ν C-OH peak area. An increase in the variety of TEG hydrogen bonding interactions was observed as the sample reached 100°C. These newly formed H-bonds were found to be just as strong as the original hydrogen bonding interactions, as the ν C-OH stretch reverted to its original wavenumber upon cooling (1076 cm^{-1}). This suggests that noticeable migration of TEG begins around 100°C, and for the purpose of ensuring uniform dispersion of TEG, a processing temperature in excess of 100°C would be required.

Upon cooling, TEG content was more homogeneously distributed across the samples, although some subtle localized domains remained. Initially the two domains were found to be sufficiently different in material properties such that two distinct glass transitions were observed. After heating and cooling, TEG was more homogeneously distributed in DBM, evident from its spatial distribution and the merging of glass transitions into one broader glass transition region.

DSC and DMA also indicated that physical aging occurred during the storage of DBM with and without TEG, but appeared to be less in the presence of TEG. This warrants further study to discern whether a plasticizer is able to inhibit aging, which is known to change the material properties of protein plastics.

ACKNOWLEDGMENTS

This research was undertaken on the infra-red microspectroscopy beamline at the Australian Synchrotron, Clayton, VIC, Australia. Proposal number AS132/IRMF1/6636. The authors would especially like to acknowledge the technical assistance of Dr. Mark Tobin and Dr. Danielle Martin. Travel funding support was received from the New Zealand Synchrotron Group.

REFERENCES

1. Verbeek, C. J. R.; Lay, M. C.; Low, A. W. K. Methods of manufacturing plastic materials from decolorized blood protein. US20130139725 A1. Application number 691,438, Waikato-link Limited: **2013**.
2. Barone, J. R.; Danganan, K.; Schmidt, W. F. *J. Agric. Food Chem.* **2006**, *54*, 5393.
3. Hicks, T.; Verbeek, C. J. R.; Lay, M. C.; Bier, J. M. *RSC Adv.* **2014**, *4*, 31201.
4. Low, A.; Verbeek, C. J. R.; Lay, M. C. *Macromol. Mater. Eng.* **2014**, *299*, 75.
5. Hicks, T. M.; Verbeek, C. J. R.; Lay, M. C.; Bier, J. M. *Macromol. Mater. Eng.* **2014**, *300*, 3, 328.
6. Bier, J. M.; Verbeek, C. J. R.; Lay, M. C. *Macromol. Mater. Eng.* **2014**, *299*, 85.
7. Low, A. *Thesis: Decoloured bloodmeal based bioplastic*. In Materials and Process Engineering; University of Waikato: Hamilton, **2012**.
8. Bourtoom, T.; Chinnan, M. S.; Jantawat, P.; Sanguandeeikul, R. *Food Sci. Technol. Int.* **2006**, *12*, 119.
9. di Gioia, L.; Guilbert, S. *J. Agric. Food Chem.* **1999**, *47*, 1254.
10. Vieira, M. G. A.; da Silva, M. A.; dos Santos, L. O.; Beppu, M. M. *Eur. Polym. J.* **2011**, *47*, 254.
11. Chen, P.; Zhang, L. *Macromol. Biosci.* **2005**, *5*, 237.
12. Bier, J. M.; Verbeek, C. J. R.; Lay, M. C. *J. Appl. Polym. Sci.* **2014**, 131.
13. Pal, S.; Kundu, T. K. *ISRN Phys. Chem.* **2013**, *2013*, 16.
14. Barth, A. *Biochim. Biophys. Acta* **2007**, *1767*, 1073.
15. Zeiss, H. H.; Tsutsui, M. *J. Am. Chem. Soc.* **1953**, *75*, 897.
16. Jeffrey, G. A. *An Introduction to Hydrogen Bonding*; Oxford University Press: New York, **1997**.
17. Singelenberg, F. A. J.; van der Maas, J. H.; Kroon-Batenburg, L. M. J. *J. Mol. Struct.* **1991**, *245*, 183.
18. Sun, C. L.; Wang, C. S. *Theochem. J. Mol. Struct.* **2010**, *956*, 38.
19. Ryu, S. R.; Noda, I.; Jung, Y. M. *Bull. Korean Chem. Soc.* **2011**, *32*, 4011.
20. Mo, X.; Sun, X. *J. Polym. Environ.* **2003**, *11*, 15.
21. Lawton, J. W.; Wu, Y. V. *Cereal Chem.* **1993**, *70*, 471.
22. Struik, L. C. E. *Physical Aging in Amorphous Polymers and Other Materials*; Elsevier: Amsterdam, **1978**, p 5.
23. Bengochea, C.; Arrachid, A.; Guerrero, A.; Hill, S. E.; Mitchell, J. R. *J. Cereal Sci.* **2007**, *45*, 275.
24. Farahnaky, A.; Badii, F.; Farhat, I. A.; Mitchell, J. R.; Hill, S. E. *Biopolymers* **2005**, *78*, 69.